PAPER

Check for updates

Effect of vacancies on the structural and electronic properties of Ti_2CO_2

Li Xiao-Hong, [iD] * Su Xiang-Ying and Zhang Rui-Zhou

Ti_2CO_2 MXene is widely considered as a potential candidate material for sensors and optical devices. In this paper, first-principles calculations are performed to investigate the structural and electronic properties of pristine and vacancy defect Ti_2CO_2 monolayer. The results indicate that C-vacancy is energetically more favorable than Ti-vacancy and O-vacancy because of the smaller formation energy of C vacancy. The introduction of vacancy defects results in the transition from semiconductor to metal, and improves the electronic conductivities of Ti_2CO_2 monolayer. The introduction of C and O vacancies causes the Ti-d state to split into several peaks in the energy range of 0 to 2 eV, while the introduction of Ti vacancy makes the Ti-d state weaker and the C-p state stronger. Furthermore, the work function can be effectively engineered by vacancy defects.

1 Introduction

Two-dimensional (2D) materials have been an active research area since the discovery of graphene.[1] Graphene is a significant 2D material[2] with zero-band gap semi-metallic properties, which hampers its application in highly integrated electronic components. We can tune the band gap of graphene, but the available range of the band gap is not enough to satisfy the requirement of the application of nanoelectronic, optoelectronic devices. Therefore, it is necessary to design or search for new layered materials with intrinsic bandgaps, high thermal stability and conductivity, and high carrier mobility.

MXene is a new group of low-dimensional materials[3–5] and has attracted intensive attention in the field of super-capacitors,[6,7] lead adsorption,[8] catalysis[9] and so on. MXene is obtained by selectively etching layers of A elements from its host, layered ternary MAX materials ($M_{n+1}AX_n$), where $n = 1, 2, 3$; M is a transition metal, and X is C or N.[10] The frequently used etchant is hydrofluoric acid (HF), HF-containing etchants and so on. F, O, and/or OH functional groups are often generated on the external surface of the exfoliated layers. So functionalized MXenes are denoted as $M_{n+1}X_nT_x$, in which T stands for the terminating F, O, and/or OH functional groups, x is the termination number.[11] These functional groups are very important in the applications of energy storage, catalysis *etc.*[12–14]

Defects have been investigated in 2D materials and can influence the performance of materials and devices.[15,16] It is important to understand the layered structure and point defects, which are crucial for exploration of the physiochemical properties of MXenes. The properties of 2D materials can be engineered by defects. For the low-dimensional materials, defects have a much stronger impact, when compared to their bulk counterparts. And defect engineering has attracted extensive attention[17] and is often used to modify the electronic structures of many layered structures.[18] Zhang *et al.*[19] theoretically investigated the carbon-vacancy ordering in Nb_4AlC_{3-x}, and reported the importance roles of carbon vacancies in the structure stability and order–disorder phase transformation. Carbon vacancies also have important influences on the superconducting properties of materials.[20–22]

Vacancies are universally present in the MAX phases.[23,24] So it is believed that MXenes inherit their hosts' defect. Ti_2CO_2 is the thinnest O-functionalized Ti-based MXene, and has many promising applications, such as catalyst, optical devices, and gas sensor.[25–27] Wang *et al.*[28] investigated the stabilities and electronic properties of vacancy-doped Ti_2CO_2. Their results indicated that the formation energies of C-vacancy are relatively small. Hu *et al.*[29] reported the influence of C-vacancy on the structural stability, electronic properties of a $2 \times 2 \times 1$ Ti_2CT_2 (T = O, F, and OH) supercell. They thought that C-vacancy in MXene is much easier to form when compared with graphene and other two-dimensional material. Bandyopadhyay *et al.*[30] investigated the structural and magnetoelectronic behavior of a $4 \times 4 \times 1$ Ti_2CO_2 supercell with single vacancy and double vacancies. They thought that the defect formation energies are greatly dependent on local chemical bonding. Sang *et al.*[31] reported the atomic defects in monolayer $Ti_3C_2T_x$ MXene. They reported that the formation energy of Ti-vacancy on $Ti_3C_2O_x$ (7.74 eV), and the defects can't strongly influence the metallic conductivity, but can influence the surface morphology and termination groups. To the best of our knowledge, limited researches report the impact of different vacancy defect on the properties of Ti_2CO_2 monolayer.

College of Physics and Engineering, Henan University of Science and Technology, Luoyang 471003, China. E-mail: lorna639@126.com
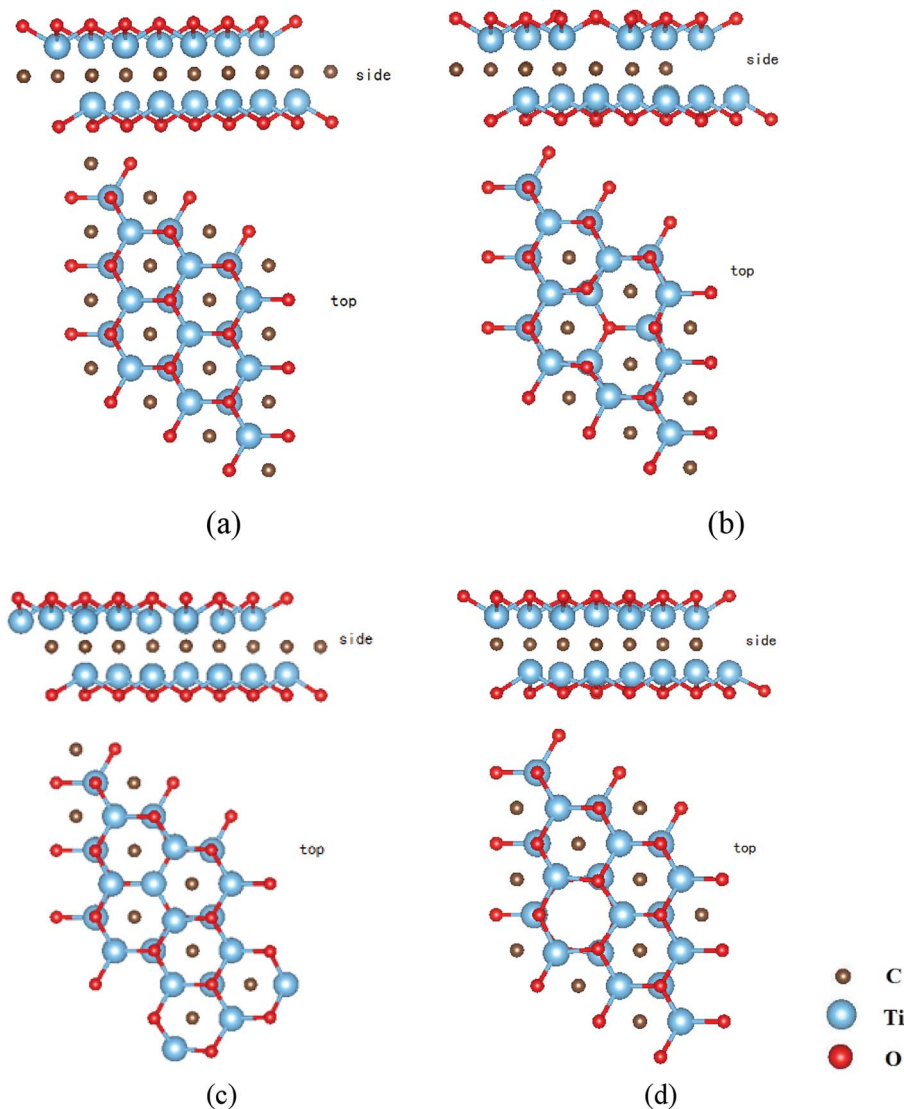
Fig. 1 The atomic structures of pristine Ti_2CO_2 (a), $Ti_2CO_2-V_{Ti}$ (b), $Ti_2CO_2-V_O$ (c), and $Ti_2CO_2-V_C$ (d) from top and side view.

Work function (WF) is an important parameter for electrode materials. A material with higher WF can be as an anode, and a material with low WF can be treated as a cathode. Research[32] indicates that the materials with higher work function can reduce the Schottky barrier, which can cause increased contact resistances and limit the performance of devices. Therefore, the modulation of WF is important to improve the device performance. Up to now, the report on the modulation of WF of Ti_2CO_2 monolayer is unavailable.

Here, we investigated the effect of carbon vacancy (V_C), Ti vacancy (V_{Ti}), and oxygen vacancy (V_O) on structure, electronic properties, and work function of Ti_2CO_2 monolayer. The comparisons of related properties between pristine and vacancy Ti_2CO_2 monolayer and the modulation of vacancy defect on WF are performed in our study, which are not discussed in other people's works.[29–31] Our investigation will provide an alternative method to engineer the physical and chemical properties of MXenes.

2 Computational details

All density functional theory (DFT) calculations are carried out using the Dmol³ code.[33] The Perdew–Burke–Ernzerhof (PBE) functional[34] generalized gradient approximation (GGA)[35] is used. The used basis set is double numerical plus polarization (DNP), which corresponds to a double-ζ quality basis set with p-type polarization functions added to hydrogen, and d-type polarization functions added to heavier atoms. DNP basis set is comparable with the Gaussian 6-31G (d, p) basis set and exhibits a better accuracy.[36] A $3 \times 3 \times 1$ Ti_2CO_2 supercell is constructed with one carbon, titanium, or oxygen removal to highlight the influence of V_C, V_{Ti}, and V_O, respectively. The three models of $Ti_2CO_2-V_C$, $Ti_2CO_2-V_{Ti}$, and $Ti_2CO_2-V_O$ monolayers are presented in Fig. 1. In order to have a comparison, the structure of pristine Ti_2CO_2 monolayer (PTM) is also presented in Fig. 1.

In order to simulate the isolated monolayer, a large vacuum space of 25 Å was set in the direction normal to MXene layers to

avoid any unnecessary interaction between the MXene layers. In our calculation, the Brillouin zone (BZ) integration was sampled by using a $5 \times 5 \times 1$ k-mesh according to Monkhorst–Pack method.[37] The convergence in energy, force and displacement were 1×10^{-6} Ha, 0.001 Ha Å^{-1}, and 0.005 Å, respectively. A denser $9 \times 9 \times 1$ mesh is used to calculate the electronic density of states (DOS).

3 Results and discussion

3.1 The structure of pristine and defect-Ti$_2$CO$_2$ monolayer

In order to determine what defects are likely to form, the vacancy formation energies E_{form} for Ti, C, or O defect are obtained by the following equation:

$$E_{form} = E_{vac} + U_{atom} - E_{pristine} \qquad (1)$$

where E_{form} is the vacancy formation energy, E_{vac} is the total energy of Ti$_2$CO$_2$ monolayer with mono-vacancy, U_{atom} is the total energy of an isolated atom, $E_{pristine}$ is the total energy of pristine Ti$_2$CO$_2$ monolayer (PTM). The calculated O-vacancy formation energy is 6.59 eV, lower than Ti-vacancy formation energy (9.67 eV), and higher than C-vacancy formation energy (5.31 eV). So C-vacancy is energetically more favorable than Ti-vacancy and O-vacancy, which is consistent with the conclusion of other researches.[29,30,38] Ti-vacancy and O-vacancy are not easy to occur when compared with C-vacancy, but they can be induced in non-equilibrium processes such as e-beam lithography,[39] which is used to decorate the vacancy defects in the MoS$_2$ monolayer.[40] Ti-vacancy deformation is more energy consuming when compared with O-vacancy and C-vacancy, which is consistent with the other researchers' results.[29,31] Sang et al.[31] reported the formation energy of Ti-vacancy on

Ti$_3$C$_2$O$_x$ (7.74 eV), which indicates that Ti-vacancy is more difficult to occur on Ti$_2$CO$_2$ monolayer (9.67 eV) than Ti$_3$C$_2$O$_x$.

The calculated crystal parameter of PTM is 9.0483 Å, while the crystal parameters of Ti$_2$CO$_2$ monolayers with Ti, C, or O defect are 9.0737, 9.0719, and 9.0636 Å, respectively. So the crystal parameters of Ti$_2$CO$_2$-V$_C$, Ti$_2$CO$_2$-V$_{Ti}$, and Ti$_2$CO$_2$-V$_O$ monolayers change slightly when compared with that of PTM. The volume of PTM is 1665.59 Å^3. Compared with the volume of PTM, the volume of Ti$_2$CO$_2$-V$_C$ monolayer increases 1.99%. The creation of C vacancy makes the Ti atoms near C vacancy away from the vacancy by the remaining strengthened pd bonds, which results in the volume increase of Ti$_2$CO$_2$-V$_C$. Compared with the volume of PTM, the volume of Ti$_2$CO$_2$-V$_{Ti}$ increases by 2.01%. The reason is that the creation of Ti vacancy makes the formation of unsaturated electrons on nearest C/O atoms, which result in the stronger interactions between C/O atoms and their nearest Ti atoms. The volume of Ti$_2$CO$_2$-V$_O$ increases by 1.90% when compared to that of PTM. The creation of O vacancy on the surface of Ti$_2$CO$_2$ monolayer makes the charge redistribution, and results in the formation of the stronger Ti–O and Ti–C bonds near O vacancy.

3.2 The electronic properties of pristine and defect-Ti$_2$CO$_2$ monolayers

Fig. 2 presents the structures of pristine and defect Ti$_2$CO$_2$ monolayer along the symmetry directions Γ–M–K–Γ. The valence band maximum (VBM) and conduction band minimum (CBM) are labelled in Fig. 2. PTM is an M–Γ indirect semiconductor with the band gap of 0.27 eV, which is close to the results of Xie et al. (0.24 eV by PBE)[41] and Zha et al. (0.261 eV by PBE).[42] The introduction of vacancy defect results in the transition from semiconductor to metal.
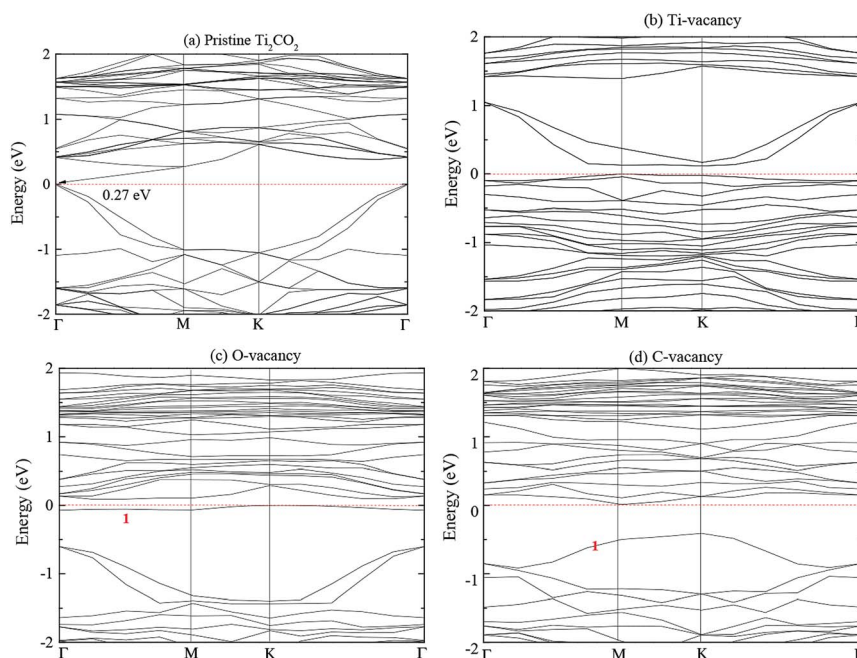

Fig. 2 The band structure of pristine and vacancy defect Ti$_2$CO$_2$ monolayer.
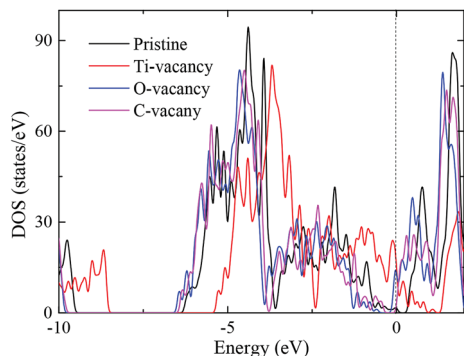
Fig. 3 The total density of states of pristine and vacancy defect Ti_2CO_2 monolayer.

Fig. 5 The work function of pristine and vacancy defect Ti_2CO_2 monolayer.

From Fig. 2(b), the introduction of Ti-vacancy makes the Fermi energy level shift downward compared with that of PTM, and the valence band passes through the Fermi level, which results in the metallic character of Ti_2CO_2-V_{Ti}. Ti defect level lies in the valence band region of PTM. From Fig. 2(c), the introduction of O vacancy defect makes the Fermi energy level shift upward. The defect energy level (band 1 in Fig. 2(c)) appears because of the removal of one oxygen atom, which passes through the Fermi energy level and results in the metallization of Ti_2CO_2-V_O. This indicates that the O vacancy has greater effect on the photocatalyst properties of Ti_2CO_2 monolayer. In addition, it is noted that the defect energy level fluctuates slightly and changes gently, which indicates that the electrons in this energy level have larger effective mass, stronger localization and electron binding. From Fig. 2(d), the introduction of
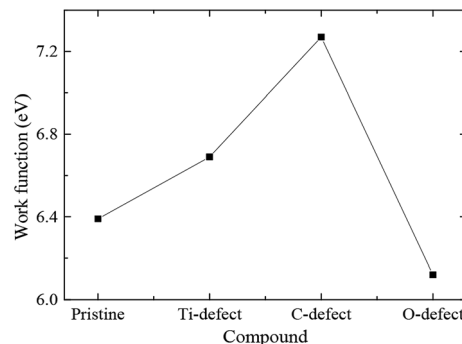
C vacancy makes the Fermi level shift upward compared with that of PTM. The defect energy level (band 1 in Fig. 2(d)) is introduced below the Fermi level. So the vacancy defect can effectively engineer the band structure of Ti_2CO_2 monolayer.

Fig. 3 presents the total density of state (DOS) of pristine and vacancy defect Ti_2CO_2 monolayer. It is noted that the introduction of vacancy defect imposes the significant impact on the electronic structure of Ti_2CO_2 monolayer. The improved electronic conductivities of Ti_2CO_2-V_{Ti}, Ti_2CO_2-V_O, and Ti_2CO_2-V_C monolayers are observed due to the significantly increased DOS at the Fermi level (E_F). So the introduction of vacancy defect can improve the electronic conductivities of functionalized MXenes.

Fig. 4 presents the partial density of state (PDOS) of Ti, O, and C atoms of vacancy defect Ti_2CO_2 monolayer in order to illustrate the origin of electronic conductivity. The PDOS of PTM
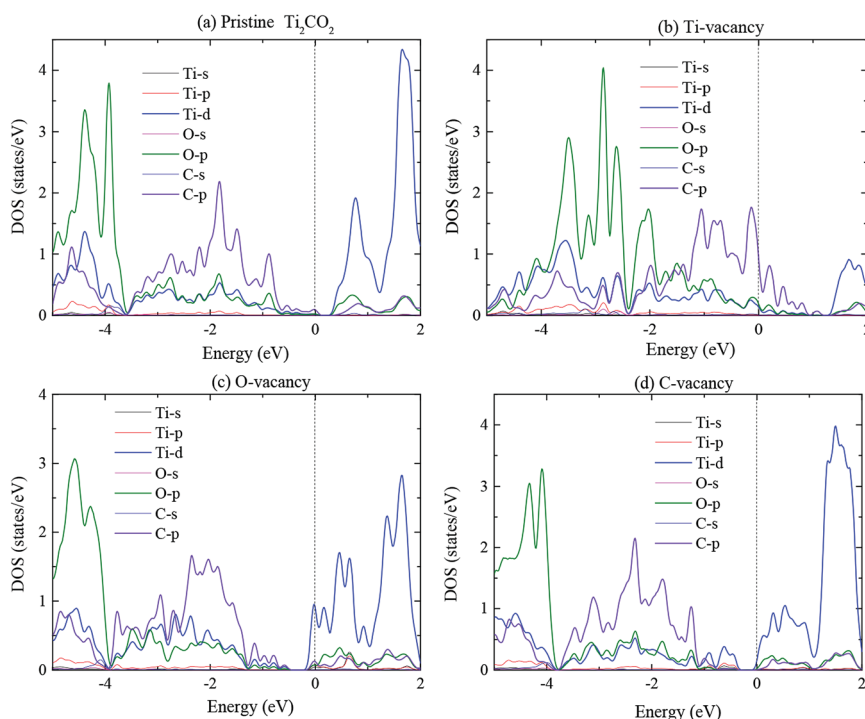

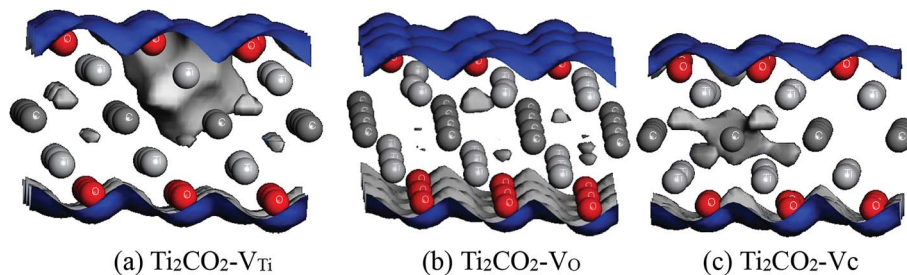**Fig. 4** The partial density of states of pristine and vacancy defect Ti_2CO_2 monolayer.

(a) Ti₂CO₂-V_Ti   (b) Ti₂CO₂-V_O   (c) Ti₂CO₂-Vc

Fig. 6 The electrostatic potentials of Ti_2CO_2-V_{Ti}, Ti_2CO_2-V_O, and Ti_2CO_2-V_C monolayers.

is also plotted in order to have a comparison. For PTM, the valence band is mainly from the contribution of Ti-d, C-p and O-p states, while the conduction band is mainly from the contribution of Ti-d states. Similar to PTM, Ti-d, O-p, and C-p states provide the mainly contribution of valence band for Ti_2CO_2-V_{Ti} monolayer, while C-p states mainly contribute to the conduction band. For Ti_2CO_2-V_O and Ti_2CO_2-V_C monolayers, Ti-d, O-p and C-p states provide the mainly contribution to valence band and conduction band. Combined Fig. 2 and 4, for Ti_2CO_2-V_{Ti} monolayer, the band at Γ point is mainly localized on C-p state, the introduction of Ti vacancy results in the unsaturated C and O atoms. For Ti_2CO_2-V_O monolayer, the introduction of O vacancy results in three unsaturated Ti-3d states, which have the main contribution to the band at Γ point. The introduction of C vacancy results in the six unsaturated Ti atoms for Ti_2CO_2-V_C monolayer, so Ti-d state have the main contribution to the band at Γ point and VBM from Fig. 4(d).

It is noted that the introduction of C and O vacancy makes Ti-d state split into several peaks in the energy range of 0 to 2 eV because of the structural modification. While the introduction of Ti vacancy makes Ti-d state weaker and C-p state stronger. Combined with Fig. 3 and 4, the valley of the total DOS at -3.5 eV in Fig. 3 is mainly from Ti-d state for Ti_2CO_2-V_{Ti} monolayer, Ti-d, O-p and C-p states for Ti_2CO_2-V_O and Ti_2CO_2-V_C monolayers. In the energy range of -3 to 0 eV, there exist strong interactions between Ti-d and C-p states, Ti-d and O-p states for all studied Ti_2CO_2 monolayers.

3.3 The analysis of work function and atomic charge

Work function (WF) is an important physical parameter of materials and plays the significant role in the light emitting diodes and the field effect transistors. The work function of pristine Ti_2CO_2 monolayer is 6.39 eV, while the work functions of Ti_2CO_2-V_C, Ti_2CO_2-V_{Ti}, and Ti_2CO_2-V_O monolayers are 7.27, 6.69, and 6.12 eV, respectively. This indicates that the work function can be effectively engineered by vacancy defect. According to the report of Ma et al.,[32] Ti_2CO_2-V_C and Ti_2CO_2-V_{Ti} monolayers with higher WFs can reduce the Schottky barrier and decrease the field emission performance, while Ti_2CO_2-V_O monolayer with lower WF can improve the field emission performance. In the other hand, Ti_2CO_2-V_C and Ti_2CO_2-V_{Ti} monolayers can be considered as anode because of the higher WFs, while Ti_2CO_2-V_O monolayer can be considered as cathode due to the lower WF (Fig. 5).

The analysis of Mulliken charge is performed in order to further investigate the effect of vacancy defect on the charge distribution. Fig. 6 presents the electrostatic potential of Ti_2CO_2-V_{Ti}, Ti_2CO_2-V_O, and Ti_2CO_2-V_C monolayers. For PTM, the charge of Ti atom in supercell is $1.202e^-$, while the charges of the adjacent C and O atoms are -0.980 and $-0.712e^-$, respectively. For Ti_2CO_2-V_{Ti} monolayer, the removal of Ti atom results in the charge localization on the defect site, adjacent unsaturated O and C atoms. The negative charge accumulation is exhibited around Ti vacancy defect. The charge aggregation is exhibited around O atoms, while the loss of negative charge is exhibited around C atoms. The charges of the adjacent C and O atoms are -0.704 and $-0.584e^-$, respectively. For Ti_2CO_2-V_O monolayer, the positive charge accumulation is exhibited around O vacancy defect. The charge of the adjacent Ti atom is $1.187e^-$, while the charge of the adjacent C atom has little change because of the longer distance from O vacancy. From Fig. 6(c), there is a clear charge accumulation around C vacancy defect for Ti_2CO_2-V_C monolayer. The charge of the adjacent Ti atom is $1.189e^-$, while the charge of adjacent O atom increases and is -0.708 e$^-$. The introduction of C vacancy weakens the adjacent Ti–O bonds.

4 Conclusion

In this paper, the structure, electronic properties of pristine and vacancy defect Ti_2CO_2 monolayer have been investigated by the first principles calculation. The analysis of formation energies indicates that C-vacancy is energetically more favorable than Ti-vacancy and O-vacancy. PTM is a semiconductor. The introduction of vacancy defect results in the metallic character of Ti_2CO_2 monolayer and improves the electronic conductivity of Ti_2CO_2 monolayer. The work function can be effectively engineered by vacancy defect. O vacancy defect can improve the field emission performance, while Ti or C vacancy defect can decrease the field emission performance for Ti_2CO_2 monolayer. The analysis of Mulliken charge is further performed.

Conflicts of interest

There are no conflicts to declare.

Acknowledgements

References

1 K. S. Novoselov, A. K. Geim, S. V. Morozov, D. Jiang, M. I. Katsnelson, I. V. Grigorieva, S. V. Dubonos and A. A. Firsov, *Nature*, 2005, **438**, 197.

2 K. S. Novoselov, D. Jiang, F. Schedin, T. J. Booth, V. V. Khotkevich, S. V. Morozov and A. K. Geim, *Proc. Natl. Acad. Sci. U. S. A.*, 2005, **102**, 10451.

3 M. Naguib, V. N. Mochalin, M. W. Barsoum and Y. Gogotsi, *Adv. Mater.*, 2014, **26**, 992.

4 Y. Gogotsi, *Nat. Mater.*, 2015, **14**, 1079.

5 M. Naguib and Y. Gogotsi, *Acc. Chem. Res.*, 2015, **48**, 128.

6 M. Ghidiu, M. R. Lukatskaya, M. Q. Zhao, Y. Gogotsi and M. W. Barsoum, *Nature*, 2014, **516**, 78.

7 M. Hu, Z. Li, G. Li, T. Hu, C. Zhang and X. Wang, *Adv. Mater. Technol.*, 2017, **2**, 1700143.

8 Q. M. Peng, J. X. Guo, Q. R. Zhang, J. Y. Xiang, B. Z. Liu, A. G. Zhou, R. P. Liu and Y. J. Tian, *J. Am. Chem. Soc.*, 2014, **136**, 4113.

9 X. Zhang, Z. Zhang, J. Li, X. Zhao, D. Wu and Z. Zhou, *J. Mater. Chem. A*, 2017, **5**, 12899.

10 M. Naguib, V. N. Mochalin, M. W. Barsoum and Y. Gototsi, *Adv. Mater.*, 2014, **26**, 992.

11 D. Magne, V. Mauchamp, S. Celerier, P. Chartier and T. Cabioch, *Phys. Rev. B: Condens. Matter Mater. Phys.*, 2015, **91**, 201409.

12 Y. Xie, M. Naguib, V. N. Mochalin, M. W. Barsoum, Y. Gogotsi, X. Yu, K.-W. Nam, X.-Q. Yang, A. I. Kolesnikov and P. R. C. Kent, *J. Am. Chem. Soc.*, 2014, **136**, 6385.

13 C. Eames and M. S. Islam, *J. Am. Chem. Soc.*, 2014, **136**, 16270.

14 Y. Xie, Y. Dall'Agnese, M. Naguib, Y. Gogotsi, M. W. Barsoum, H. L. Zhuang and P. R. C. Kent, *ACS Nano*, 2014, **8**, 9606.

15 R. Bourrellier, S. Meuret, A. Tararan, O. Stéphan, M. Kociak and L. H. G. Tizei, *Nano Lett.*, 2016, **16**, 4317.

16 D. Wong, J. Velasco, L. Ju, J. Lee, S. Kahn, H.-Z. Tsai, C. Germany, T. Taniguchi, K. Watanabe, A. Zettl, F. Wang and M. F. Crommie, *Nanotechnol*, 2015, **10**, 949.

17 T. T. Tran, K. Bray, M. J. Ford, M. Toth and I. Aharonovich, *Nat. Nanotechnol.*, 2015, **11**, 37.

18 W. M. Parkin, A. Balan, L. Liang, P. M. Das, M. Lamparski, C. H. Naylor, J. A. RodriguezManzo, A. T. Johnson, V. Meunier and M. Drndic, *ACS Nano*, 2016, **10**, 4134.

19 H. Zhang, T. Hu, X. H. Wang, Z. J. Li, M. M. Hu, E. D. Wu and Y. C. Zhou, *Sci. Rep.*, 2015, **5**, 14192.

20 A. I. Gusev, *Disorder and Order in Strongly Nonstoichiometric Compounds: Transition Metal Carbides, Nitrides and Oxides*, Springer, New York, 2001.

21 J. Nguyen, N. Glandut, C. D. Jaoul and P. Lefort, *Langmuir*, 2013, **29**, 12036.

22 X. X. Yu, G. B. Thompson and C. R. Weinberger, *J. Eur. Ceram. Soc.*, 2015, **35**, 95.

23 H. Wang, H. Han, G. Yin, C.-Y. Wang, Y.-Y. Hou, J. Tang, J.-X. Dai, C.-L. Ren, W. Zhang and P. Huai, *Materials*, 2017, **10**(2), 103.

24 H. Han, D. Wickramaratne, Q. Huang, J. X. Dai, T. W. Li, H. Wang, W. Zhang and P. Huai, *RSC Adv.*, 2016, **6**, 84262.

25 X.-F. Yu, Y.-C. Li, J.-B. Cheng, Z.-B. Liu, Q.-Z. Li, W.-Z. Li, X. Yang and B. Xiao, *ACS Appl. Mater. Interfaces*, 2015, **7**, 13707.

26 X.-F. Yu, J.-B. Cheng, Z.-B. Liu, Q.-Z. Li, W.-Z. Li, X. Yang and B. Xiao, *RSC Adv.*, 2015, **5**, 30438.

27 X. Zhang, Z. Zhang, J. Li, X. Zhao, D. Wu and Z. Zhou, *J. Mater. Chem. A*, 2017, **5**, 12899.

28 C. Wang, H. Han and Y. Guo, *Comput. Mater. Sci.*, 2019, **159**, 127.

29 T. Hu, J. Yang and X. Wang, *Phys. Chem. Chem. Phys.*, 2017, **19**, 31773.

30 A. Bandyopadhyay, D. Ghoshb and K. Swapan Pati, *Phys. Chem. Chem. Phys.*, 2018, **20**, 4012.

31 X. Sang, Y. Xie, M. W. Lin, M. Alhabeb, K. L. Van Aken, Y. Gogotsi, P. R. Kent and K. Xiao, *ACS Nano*, 2016, **10**, 9193.

32 Y. Ma, C. Shen, A. Zhang, L. Chen, Y. Liu, J. Chen, Q. Liu, Z. Li, R. M. Amer, T. Nilges, N. Ahmad Abbas and C. Zhou, *ACS Nano*, 2017, **11**, 7126.

33 B. Delley, *J. Chem. Phys.*, 1990, **92**, 508.

34 J. P. Perdew, K. Burke and M. Ernzerhof, *Phys. Rev. Lett.*, 1996, **77**, 3865.

35 P. E. Blöchl, *Phys. Rev. B: Condens. Matter Mater. Phys.*, 1994, **50**, 17953.

36 M. Wang, H. Liu, Z.-H. Huang and F. Kang, *Chem. Eng. J.*, 2014, **256**, 101.

37 H. J. Monkhorst and J. D. Pack, *Phys. Rev. B: Solid State*, 1976, **13**, 5188.

38 H. Han, D. Wickramaratne, Q. Huang, J. X. Dai, T. W. Li, H. Wang, W. Zhang and P. Huai, *RSC Adv.*, 2016, **6**, 84262.

39 J. M. Gibson, *Phys. Today*, 1997, **50**, 56.

40 H. P. Komsa, J. Kotakoski, S. Kurasch, O. Lehtinen, U. Kaiser and A. V. Krasheninnikov, *Phys. Rev. Lett.*, 2012, **109**, 035503.

41 Y. Xie and P. R. C. Kent, *Phys. Rev. B: Condens. Matter Mater. Phys.*, 2013, **87**, 235441.

42 X.-H. Zha, K. Luo, Q. Li, Q. Huang, J. He, X. Wen and S. Du, *Europhys. Lett.*, 2015, **111**, 26007.